TECHNICAL TRANSACTIONS | CZASOPISMO TECHNICZNE
CIVIL ENGINEERING | BUDOWNICTWO
2-B/2015

PIOTR GÓRSKI*, MARCIN TATARA*, STANISLAV POSPIŠIL**,
SERGEJ KUZNETSOV**, ANTE MARUŠIĆ***

INVESTIGATIONS OF STROUHAL NUMBERS OF ICED CABLE MODELS OF CABLE-SUPPORTED BRIDGES WITH RESPECT TO ANGLE OF WIND ATTACK

BADANIA LICZB STROUHALA MODELI OBLODZONYCH CIĘGIEN MOSTÓW PODWIESZONYCH Z UWZGLĘDNIENIEM KĄTA NATARCIA WIATRU

Abstract

The influence of the ice accretion, angle of attack and *Reynolds* number on the flow field around iced cables of cable-supported bridges is not clearly understood. The Strouhal number is one of the most important parameters which is necessary for an analysis of the vortex excitation response of slender structures. This paper presents the method and results of wind tunnel investigations of the Strouhal number of stationary iced cable models of cable-supported bridges. The investigations were conducted in a climatic wind tunnel laboratory of the Czech Academy of Sciences in Telč. The methodology leading to the experimental icing of the inclined cable model in the climatic section of the laboratory was prepared. The shape of the ice on the cable was registered by photogrammetry and numerical evaluation. For the aerodynamic investigations, the iced cable model in a smaller scale was reproduced using a 3D printing procedure. The Strouhal number was determined within the range of the Reynolds number between $2.4 \cdot 10^4$ and $16.4 \cdot 10^4$, based on the dominant vortex shedding frequency measured in the flow behind the model. The model was orientated at three principal angles of wind attack for each of the Reynolds number values. In order to recognize the tunnel blockage effect, the Strouhal number of a smooth circular cylinder was tested. Strong agreement with the generally reported value in the subcritical Reynolds number range for a circular cylinder was obtained.

Keywords**:** *bridge cable, ice accretion, Strouhal number, angle of attack, vortex shedding frequency*

Streszczenie

Wpływ oblodzenia, kąta natarcia wiatru i liczby Reynoldsa na zjawisko opływu powietrza wokół oblodzonych cięgien mostów podwieszonych nie został dotychczas dobrze poznany. Liczba Strouhala jest jednym z ważniejszych parametrów, którego znajomość jest niezbędna na etapie analizy odpowiedzi smukłych konstrukcji na wzbudzenie wirowe. W artykule przedstawiono sposób i wyniki badań liczby Strouhala nieruchomych modeli oblodzonych cięgien mostów podwieszonych. Badania wykonano w tunelu aerodynamicznym z komorą klimatyczną Laboratorium Czeskiej Akademii Nauk w Telč. W komorze klimatycznej wykonano doświadczalne oblodzenie modelu cięgna o osi nachylonej pod kątem 30° do płaszczyzny poziomej. Kształt oblodzonej powierzchni zarejestrowano metodą fotogrametrii cyfrowej. Do badań w tunelu aerodynamicznym wykonano nowy model sekcyjny oblodzonego cięgna metodą druku 3D. Liczbę Strouhala wyznaczono w zakresie wartości liczby Reynoldsa od $2{,}4 \cdot 10^4$ do $16{,}4 \cdot 10^4$ na podstawie pomiaru częstości odrywania się wirów w śladzie aerodynamicznym za modelem. Badania wykonano przy trzech podstawowych kierunkach napływającego powietrza. W celu określenia wpływu zjawiska blokowania tunelu na wyniki pomiarów wykonano badanie liczby Strouhala gładkiego walca kołowego. Otrzymane wartości były zgodne z wartościami podanymi w literaturze przedmiotu w zakresie podkrytycznym liczby Reynoldsa.

Słowa kluczowe: cięgno, oblodzenie, liczba Strouhala, kąt natarcia, częstość wzbudzenia wirowego

DOI: 10.4467/2353737XCT.15.147.4184

* Department of Road and Bridges, Opole University of Technology, Poland.
** Institute of Theoretical and Applied Mechanics, Academy of Sciences of the Czech Republic, Czech Republic.
*** Faculty of Mechanical Engineering and Naval Architecture, University of Zagreb, Croatia.

1. Introduction

The excitation mechanism of cables on cable-supported bridges and associated boundary conditions are described in a paper by Flaga and Michałowski [5]. A complete analysis of the dynamic wind response of such structures requires that the along wind response, vortex excitation response and lateral turbulence component response should be evaluated. Such phenomena become more significant especially for cables longer than 100 m. Theoretical background and proposals of the mathematical description of wind excitation components are presented in the respective monographs Flaga [3, 4].

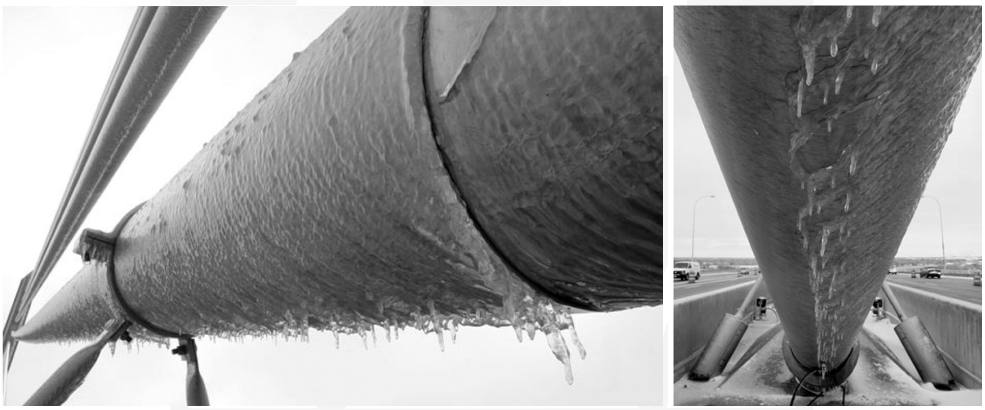

Fig. 1. Example of the iced cable of cable-supported Veteran's Glass City Skyway Bridge in Toledo, Ohio, USA [11]

The change of the cross-section of the cable due to ice accretion (see Fig. 1) has a significant influence on the flow field around the cables and its aerodynamics. In this case, an asymmetric airflow around the cable appears; thus, an asymmetric distribution of wind pressure exists on its surface. For this reason, three aerodynamic coefficients, i.e. drag, lift and moment coefficients, depending on the angle of the wind attack, should be taken into account. Moreover, in such conditions, an aeroelastic instability of the iced cable known as galloping instability may occur if the specific criteria proposed by Den Hartog [9] are met. It is well documented that the amplitude of the galloping of ice accreted cables or transmission lines can be very large [7, 8, 16].

Analysis of the vortex excitation response of the iced cables requires, among other things, knowledge of the Strouhal number – this characterizes the vortex shedding frequency. The value of Strouhal number depends on the icing shape accreted on the cable under specific conditions, structural motion and turbulence intensity, and in some cases, may depend on the Reynolds number determining the flow regimes for structures with a circular cross-section. Knowledge of the Strouhal number is necessary for the determination of critical wind velocity at which the largest amplitudes due to vortex excitation are observed.

Specific papers exist concerning modelling the icing of power lines [13], identification of amplitudes of wind induced vibrations [8] as well as investigations of the Strouhal number of iced electrical power cables [14] in scientific literature. However, because of the relative small outer diameter of electrical power cables (which do not exceeded several centimetres) as well as different shapes of the ice formations, the results are inappropriate for cables of cable-supported bridges due to their larger diameters, usually between 10 and several tenths of centimetres. Investigations of ice shaping and its influence on the aerodynamics of iced circular cylinders with diameters of 7.0 and 8.9 cm were presented in the papers by Gjelstrup et al. [7] and Koss et al. [12]; however, the Strouhal number was not investigated. Extensive studies of ice accretion processes and the final shapes of ice accreted on vertical and inclined cable models (cable diameter – 16.0 cm) were described in a paper by Demartino et al. [1]. In the paper, the aerodynamic force coefficients were also measured and it was found that they were significantly affected by the characteristics of the ice accretion.

This paper presents the method and results of wind tunnel investigations of the Strouhal number of a stationary iced cable model with respect to different angles of wind attack. The experiments were carried out in the climatic wind tunnel laboratory of the Czech Academy of Sciences in Telč (http://cet.arcchip.cz/wind-laboratory-en) using the rain sprinklers simulating the real situation during freezing rain conditions. The methodology leading to the experimental icing of the inclined cable model in the climatic section of the laboratory was prepared. The shape of the ice on the cable was registered by the photogrammetry method with the combination of numerical image analysis. For the aerodynamic investigations, the iced cable model was reproduced to a smaller scale with a 3D printing procedure. The Strouhal number was determined within the range of the Reynolds number between $2.4 \cdot 10^4$ and $16.4 \cdot 10^4$ based on the dominant vortex shedding frequency measured in the flow behind the model. The model was orientated at three principal angles of wind attack for selected values of the Reynolds number. To recognize the tunnel blockage effect, the Strouhal number of a circular smooth cylinder was tested. A good agreement with the generally reported value in the subcritical Reynolds number range for a circular cylinder was obtained.

2. The icing process of the cable model in the climatic section of the wind tunnel

The climatic section of the laboratory is combined as a closed circuit with the aerodynamic section. The climatic section has a rectangular cross-section which is 2.5 m in height, 3.9 m in width and 9.0 m in length. Using the cooling or heating system, the air temperature can be manipulated from -5°C to +30°C in a relatively short time period. In this section, the wind velocity ranges from 0.8 to 18 m/s (depending on the position of the vertically moveable ceiling and flow nozzle). The rain intensity together with the size of drops may be regulated to simulate effects corresponding to drizzle or heavy rain.

The experimental icing of the cable section model using a pipe with a 0.160 m diameter and 2.5 m length was conducted. The cable model was made of polyvinyl chloride (PVC), the outer surface structure of which was similar to the real surface of the cable cover made of high-density polyethylene (HDPE). The cable model was inclined at 30° and fixed to a special frame with the possibility of rotation relative to the airflow (Fig. 2).

Fig. 2. View of the support of the cable model on the special frame placed in the climatic section of the wind tunnel

Different types of ice can occur in different climatic conditions, i.e. with different combinations of temperature, wind velocity, angle of wind attack and droplets of the rain. For the purpose of this research, the most common natural conditions expected for a Central-European climate were selected, causing smooth evenly distributed ice accretion together with frozen rivulets on the cable for light rain, relatively low wind velocity (the droplets are able to attach the cooled cross-section) and a temperature slightly below 0°C. Another reason for this selection was to ensure an appropriate horizontal velocity component of the water droplets. Thus, the boundary conditions during the test were as follow: mean wind velocity 2.8 m/s; air temperature slightly below 0°C; diameter of the sprinkler heads – 2.8 mm. After several preliminary tests, a 40 min cooling exposure time period was selected as sufficient from the point of view of ice creation (no significant changes of ice shape occurred). During the experiment, the model was inclined on a horizontal plane to the airflow direction at an angle of 60°. The angle was found from several preliminary tests as the one at which the ice ribs on the underside of the model were much more distinctive. Before the test, several precooling procedures of the cable model were tested. Finally, the procedure using dry ice placed inside the tube was selected because this proved to be the most effective. In this case, the ice accreted on the cable was classified as a glaze dominant type of ice.

The final ice shape on the cable (see Fig. 3) was compared to Fig. 1 as the reference. The characteristic ice ribs (frozen rivulets on the underside of the model) were created and used for further examination. On the upper part of the model, the ice shape was similar to the circular shape. The cross-section of the cable with ice became strongly nonsymmetrical having dimensions of 0.192 m in height and 0.181 m in width.

It should be noticed that the cooling and icing procedure was carried out on a scale of 1:1; thus, no scaling factors were considered. Surface (roughness, material) effect on the flow around the cable during icing procedure is negligible because of low wind velocity, also, relatively large drops were simulated and the effect of the flow deflection near the surface of the cable on drop trajectory is negligible. The largest effect of the surface was with regard to water run-off – both the real surface and cable model surface behaved very similarly in this regard.

Fig. 3. Final icing effect of the cable model in climatic section (view from the bottom of the model)

3. Preparation of iced cable model for wind tunnel investigations

After the tests in the climatic section, the shape of the iced cable model was registered by a photogrammetry method with the combination of numerical image analysis. This method was realized by taking a series of 35 photographs at a distance of 1.2 m from the model. For taking the photographs, a Nikon D600 camera with a Nikon 50 mm f/1.4 AF-S lens was used for which the angular position was changed by about 9° around the model. The positions of the camera are shown in Fig. 4. In order to achieve the best results during the process of photogrammetry, the surface of the ice was painted white before taking photographs.

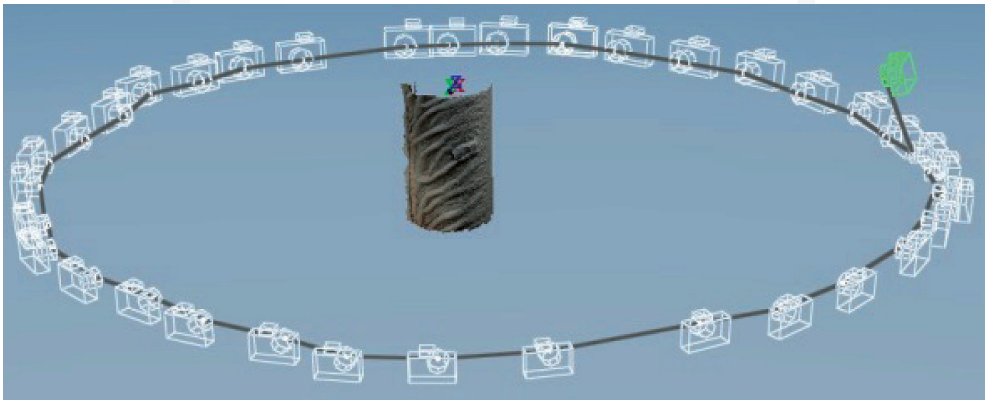

Fig. 4. Positions of the camera during a series of 35 photographs of the iced cable model

Based on the numerical image analysis of all photographs, a three-dimensional numerical model of the iced cable was obtained (Fig. 5a). For the wind tunnel investigations of the Strouhal number, the new iced cable model, shown in Fig. 5b, was made at a scale of 1:1.6 using a 3D printing procedure. The new model 0.43 m long and was constructed from polylactide plastic (PLA) – this is a standard material used for 3D printing. The dimensions of the cross-section of the new iced cable model were 0.120 m high and 0.113 m wide (see Fig. 7).

The roughness of the printed model (due to 3D printer resolution) can be neglected because the roughness caused by the ice shape (on the upper side by frozen drops, on the lower side by ice ridges) is of an order of magnitude bigger and is therefore dominant with respect to the flow characteristics. The 3D printed iced cable model has a rough shape with a surface roughness of 18% in the form of ice rivulets (covering about 150°) and 0.73% as small ice accretion on the rest of the surface of the cable model.

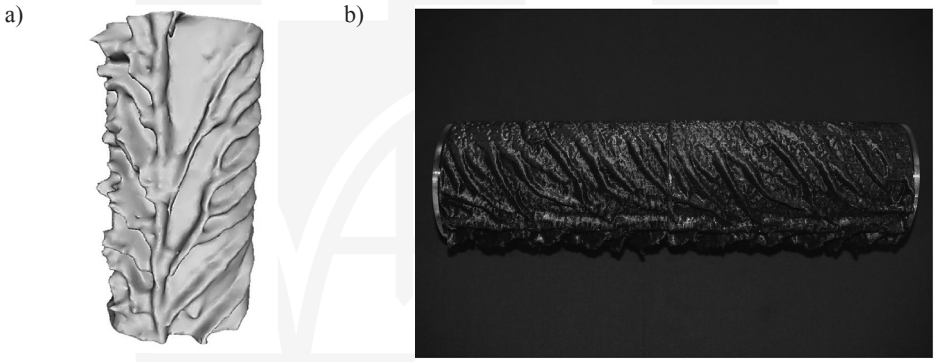

Fig. 5. a) Three-dimensional model of the iced cable; b) iced cable model for wind tunnel investigations made using 3D printing method

4. Strouhal number investigations in aerodynamic section

The Strouhal number investigations were carried out in the aerodynamic section of the wind tunnel. This section has a height of 1.8 m, and a width of 1.9 m. The flow development section is 11.0 m long to assure the appropriate simulation of the atmospheric boundary layer. The wind velocity ranges from 1.5 to 33 m/s.

During the tests, the flow was modelled as laminar with a turbulence intensity in the order of 3 %. The air temperature was in the range 24°C to 28°C. The tests were carried out at twelve sequential free stream velocities in the range 3.4 m/s to 22.9 m/s. This corresponded to the twelve Reynolds number regimes in the interval $Re = 2.4 \cdot 10^4$ to $16.4 \cdot 10^4$.

The cable with the ice model was fixed horizontally at a height of 76 cm above the floor of the aerodynamic section, perpendicular to the airflow within a special frame. Two sides of the frame were equipped with plexi-glass end-plates to ensure a two-dimensional flow around the model. The model connection to the special frame in the aerodynamic section is shown in Fig. 6.

The Strouhal effect was experimentally ascertained and analysed during three test series in which the iced cable model was orientated at three different angles of wind attack for each of the Reynolds number values. The principal model configurations and reference dimension d perpendicular to the wind direction are shown in Fig. 7.

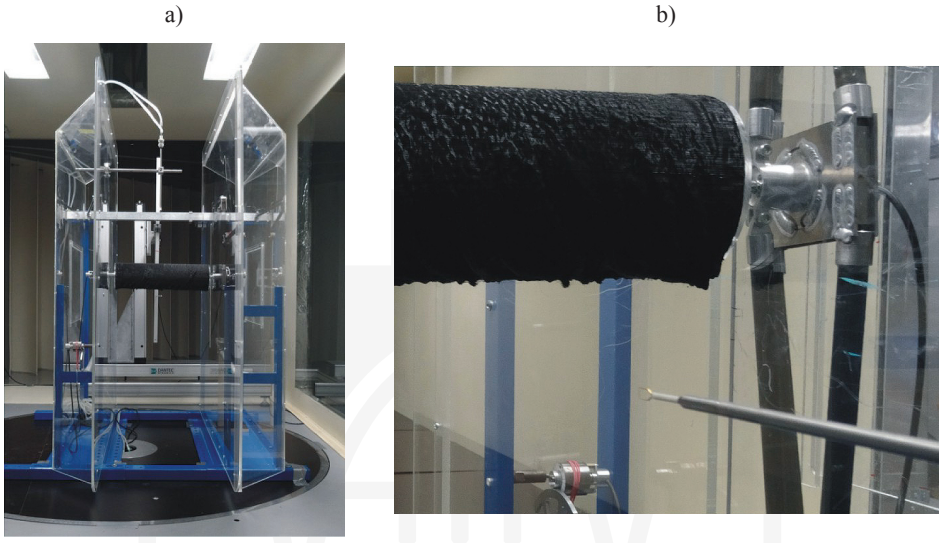

Fig. 6. a) View of the special frame with the iced cable model in aerodynamic section; b) view of the model connection to the frame and the hot-wire anemometer CTA behind the model

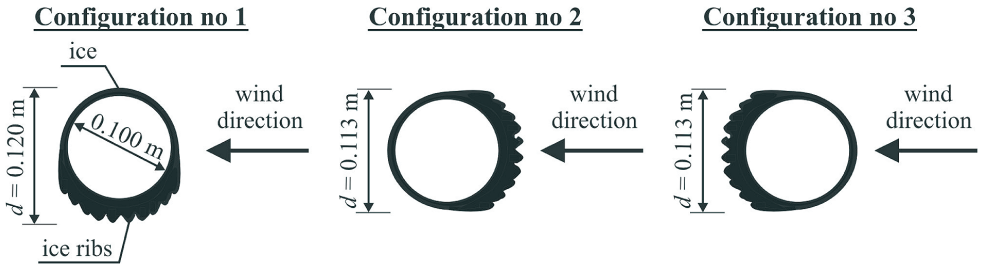

Fig. 7. Model configurations and their reference dimension d perpendicular to the wind direction considered for Strouhal number investigations

The Strouhal number was investigated according to the following procedure. At each step during the tests, the free stream velocity u in front of the model was measured by the Prandtl's tube. At the same time, the airflow velocity at a distance of about $1.5 \cdot d$ to $2.5 \cdot d$ (15 to 25 cm) behind the model was also measured by two hot-wire anemometers (CTA) during the 30 s interval with a sampling rate of 1000 Hz. Two CTA were fixed exactly 10 cm above and below the longitudinal axis of the model.

The Strouhal number was determined from the dominant vortex shedding frequency f_s that was evaluated on the basis of the power spectral density (PSD) of the airflow velocity behind the model.

The Strouhal number was calculated from the formula:

$$\mathrm{St} = \frac{f_s \cdot d}{\overline{u}} \tag{1}$$

where f_s is the vortex shedding frequency, d is the reference dimension of the iced model perpendicular to the wind direction (see Fig. 7) and $\overline{u}$ is the mean free stream velocity in front of the model.

The Reynolds number was evaluated according to the formula:

$$\mathrm{Re} = \frac{d \cdot \overline{u}}{\vartheta} \tag{2}$$

where $\vartheta = 1.64 \cdot 10^{-5}$ to $1.67 \cdot 10^{-5}$ m^2/s is the kinematic viscosity of the air.

In the wind tunnel investigations, the possibility of the tunnel blockage effect should be taken into account. In order to recognize if the blockage effect has any influence on the test results, the Strouhal number of the circular smooth cylinder was initially investigated. The diameter of the cylinder was 0.10 m and the mean free stream velocity during the test was $\overline{u}$ = 15.0 m/s. The cylinder model was fixed in the same manner as the iced model (Fig. 8a). Fig. 8b shows the PSD of the airflow velocity behind the circular cylinder model which corresponds to the mean free stream velocity of $\overline{u}$ = 15.0 m/s. The obtained Strouhal number value St = 0.18 equals that proposed in Eurocode [2]. Thus, no detrimental blockage effect of the tunnel was observed.

a)

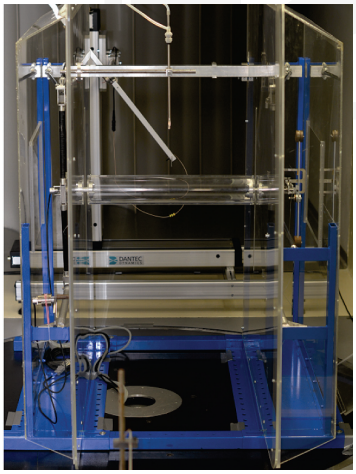

b)

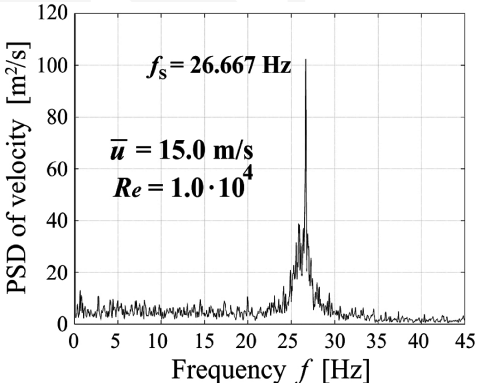

Fig. 8. a) View of the circular smooth cylinder in the special frame; b) the PSD of the airflow velocity behind the cylinder

5. Results of Strouhal number investigations for configuration no. 1

Fig. 9 depicts the selected PSDs of the airflow velocity behind the iced cable model for configuration no 1 (see Fig. 7), measured by CTA below the model at the mean free stream velocity from $\overline{u}$ = 3.5 m/s to $\overline{u}$ = 20.8 m/s. The differences between the dominant vortex shedding frequencies measured above and below the model did not exceed 5% – this is considered to be satisfactory.

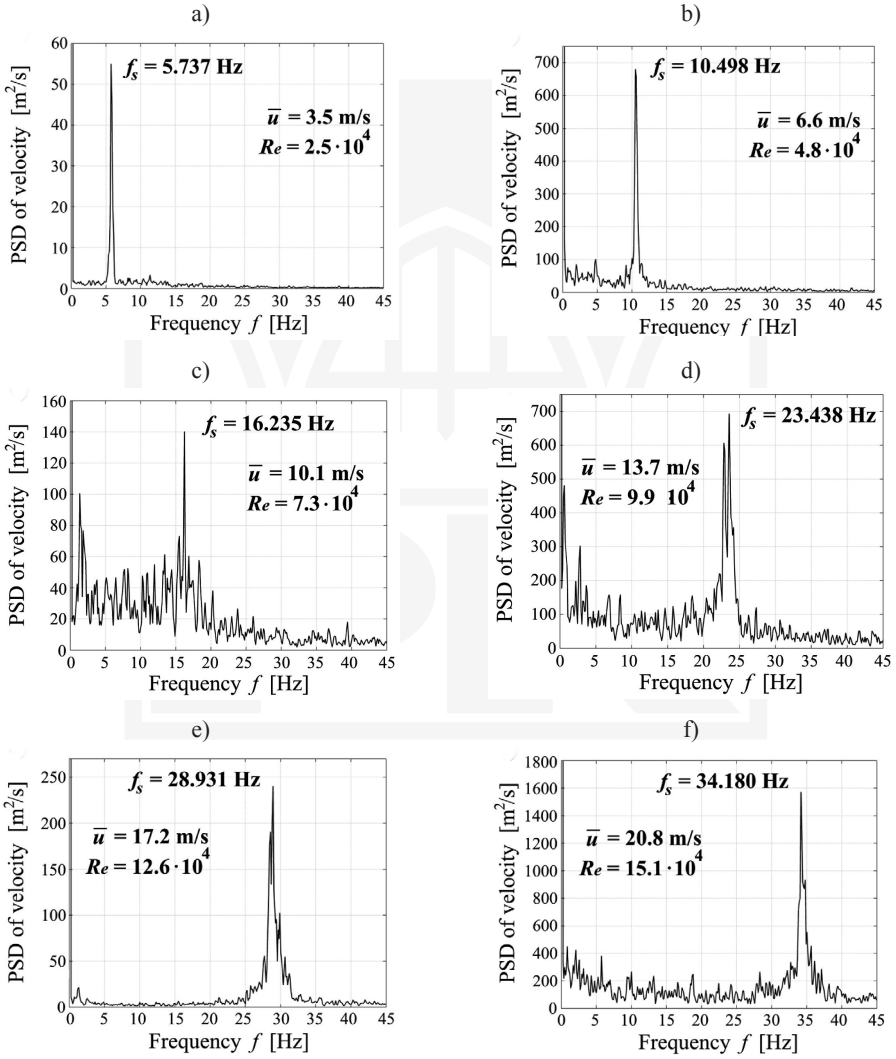

Fig. 9. Selected PSDs of the airflow velocity behind the iced cable model and dominant vortex shedding frequencies f_s for configuration no 1 correspond to the mean free stream velocities: a) $\overline{u}$ = 3.5 m/s, b) $\overline{u}$ = 6.6 m/s, c) $\overline{u}$ = 10.1 m/s, d) $\overline{u}$ = 13.7 m/s, e) $\overline{u}$ = 17.2 m/s, f) $\overline{u}$ = 20.8 m/s

Fig. 10 shows the variation of the vortex shedding frequency f_s with the mean free stream velocity $\overline{u}$. Fig. 11 depicts the variation of the Strouhal number with the Reynolds number values for configuration no. 1.

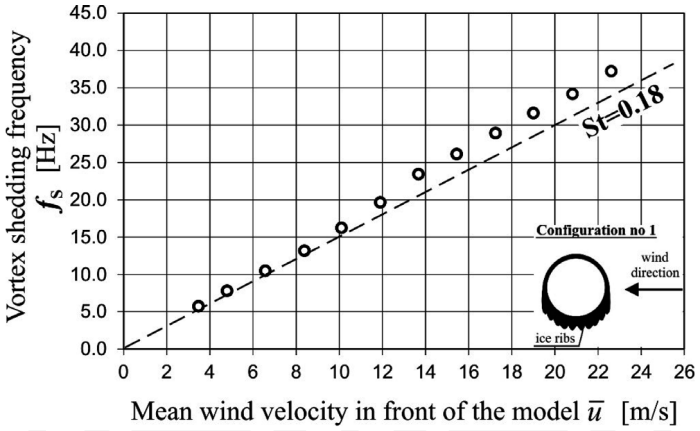

Fig. 10. Variation of the vortex shedding frequency f_s with the mean free stream velocity $\overline{u}$ in front of the model for configuration no. 1 with reference to St = 0.18 (dotted line)

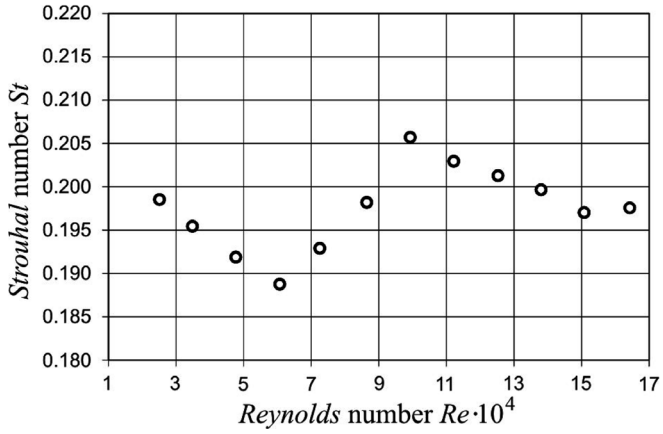

Fig. 11. Variation of the Strouhal number with the Reynolds number for configuration no 1

6. Results of Strouhal number investigations for configuration no. 2

Fig. 12 shows the selected PSDs of the airflow velocity behind the iced cable model for configuration no. 2, measured by CTA below the model at the mean free stream velocity from $\overline{u}$ = 3.4 m/s to $\overline{u}$ = 20.9 m/s. As in the previous case, the differences between the dominant

vortex shedding frequencies obtained from the measurements using CTA located above and below the model did not exceed 5%.

Fig. 13 shows the variation of the vortex shedding frequency f_s with the mean free stream velocity $\overline{u}$. Fig. 14 depicts the variation of the Strouhal number with the Reynolds number values for configuration no. 2.

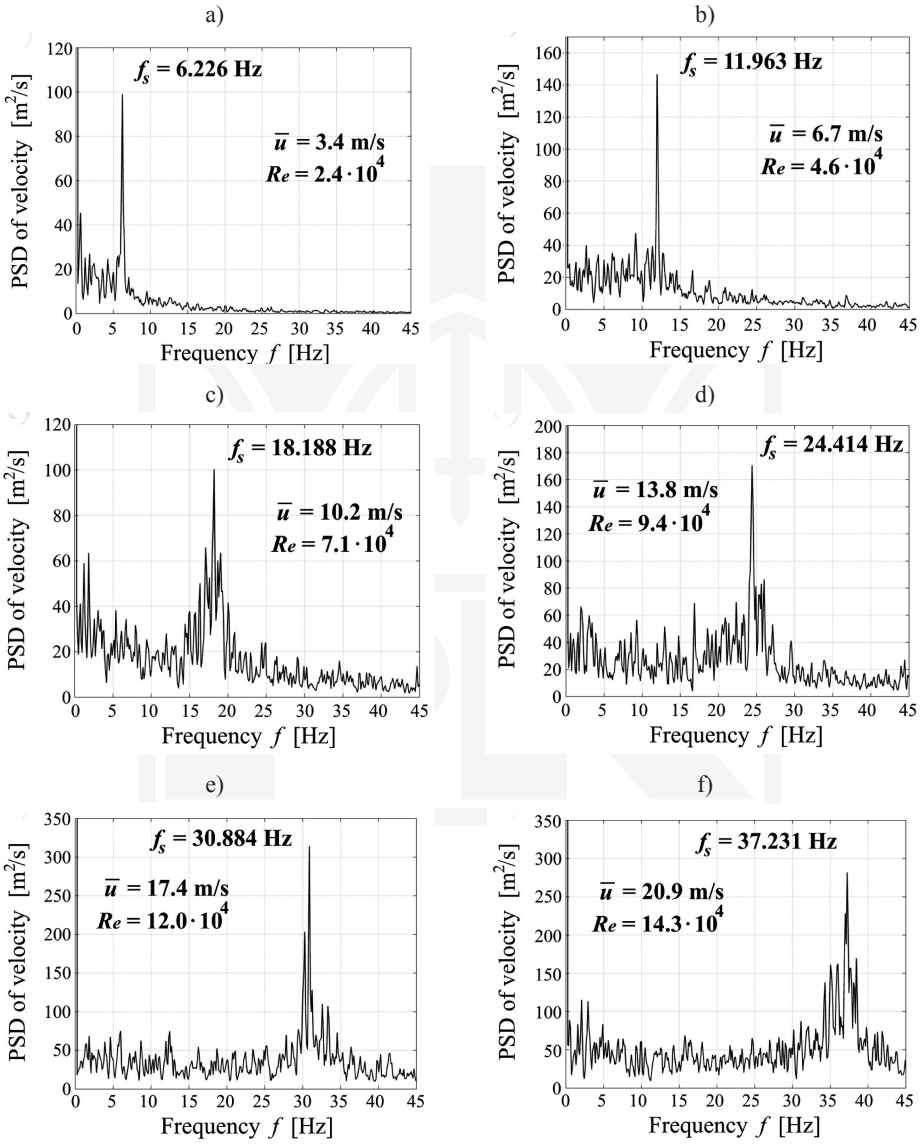

Fig. 12. Selected PSDs of the airflow velocity behind the iced cable model and dominant vortex shedding frequencies f_s for configuration no. 2 correspond to the mean free stream velocities: a) $\overline{u}$ = 3.4 m/s, b) $\overline{u}$ = 6.7 m/s, c) $\overline{u}$ = 10.2 m/s, d) $\overline{u}$ = 13.8 m/s, e) $\overline{u}$ = 17.4 m/s, f) $\overline{u}$ = 20.9 m/s

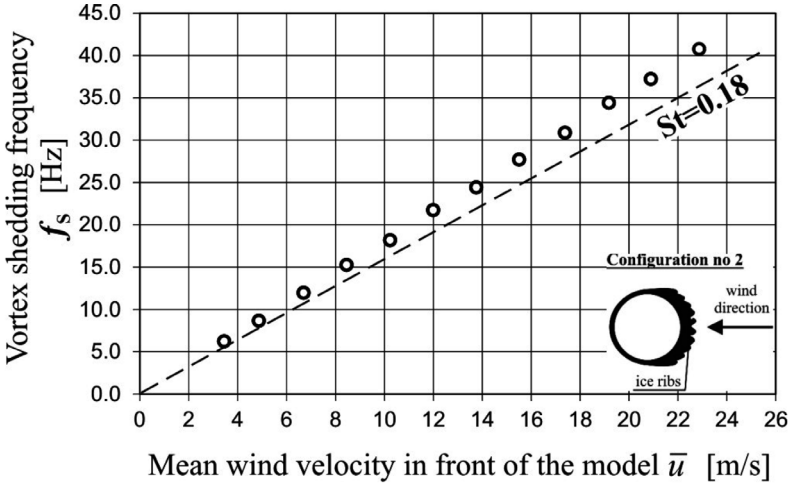

Fig. 13. Variation of the vortex shedding frequency f_s with the mean free stream velocity $\overline{u}$ in front of the model for configuration no. 2 with reference to St = 0.18 (dotted line)

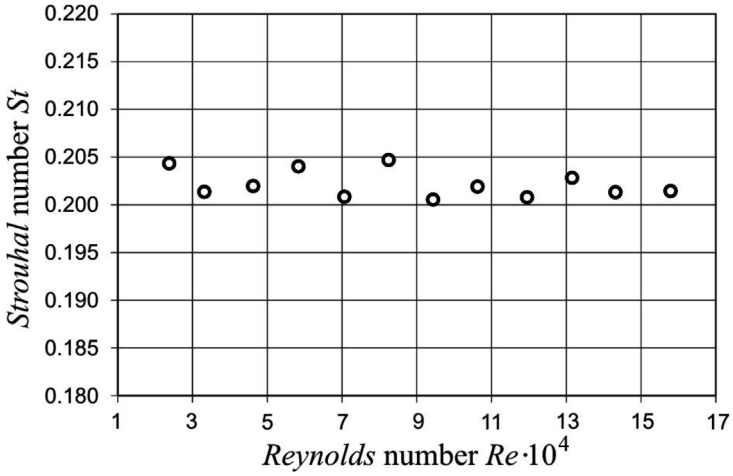

Fig. 14. Variation of the Strouhal number with the Reynolds number for configuration no. 2

7. Results of Strouhal number investigations for configuration no. 3

Fig. 15 shows the selected PSDs of the airflow velocity behind the iced cable model for configuration no 3 at the mean free stream velocity from $\overline{u}$ = 3.5 m/s to $\overline{u}$ = 21.0 m/s. The differences between the dominant vortex shedding frequencies obtained from the measurements using CTA located above and below the cylinder did not exceed 6%.

Fig. 16 shows the variation of the vortex shedding frequency f_s with the mean free stream velocity $\overline{u}$. Fig. 17 depicts the variation of the Strouhal number with the Reynolds number values for configuration no. 3.

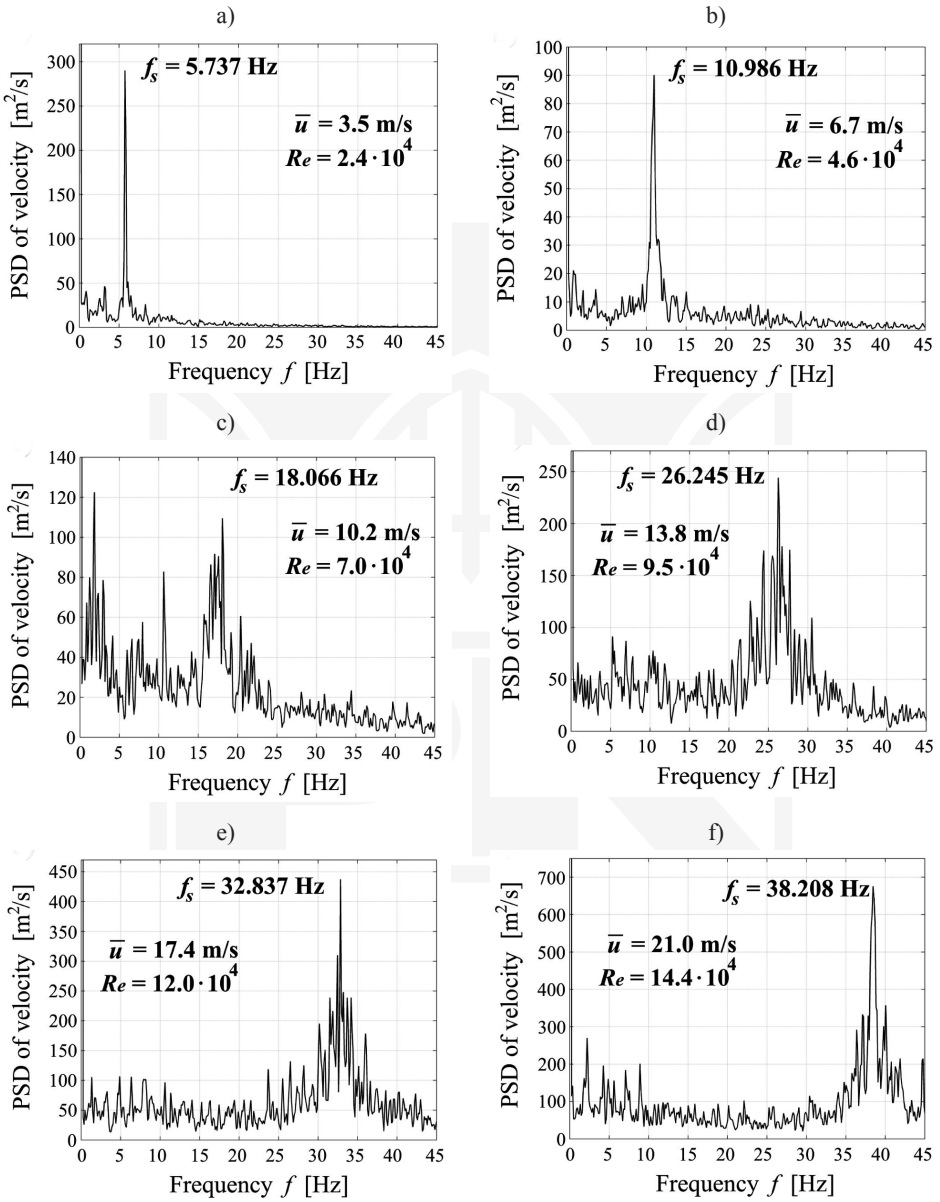

Fig. 15. Selected PSDs of the airflow velocity behind the iced cable model and dominant vortex shedding frequencies f_s for configuration no. 3 correspond to the mean free stream velocities: a) $\overline{u}$ = 3.5 m/s, b) $\overline{u}$ = 6.7 m/s, c) $\overline{u}$ = 10.2 m/s, d) $\overline{u}$ = 13.8 m/s, e) $\overline{u}$ = 17.4 m/s, f) $\overline{u}$ = 21.0 m/s

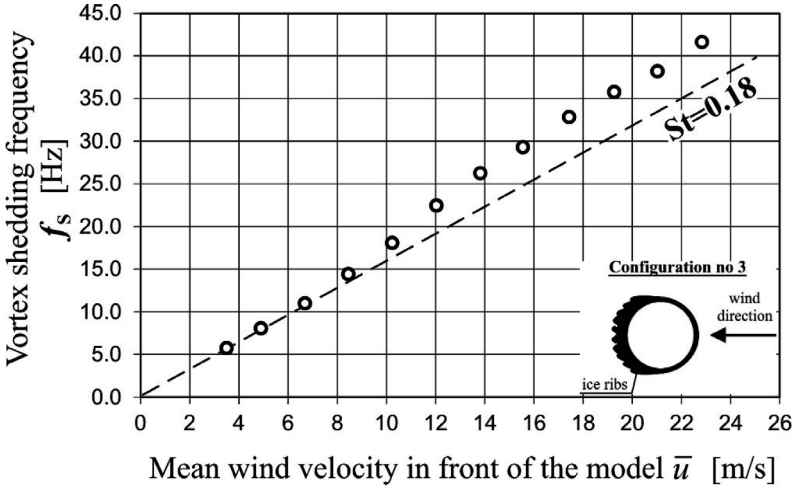

Fig. 16. Variation of the vortex shedding frequency f_s with the mean free stream velocity $\overline{u}$ in front of the model for configuration no 3 with reference to St = 0.18 (dotted line)

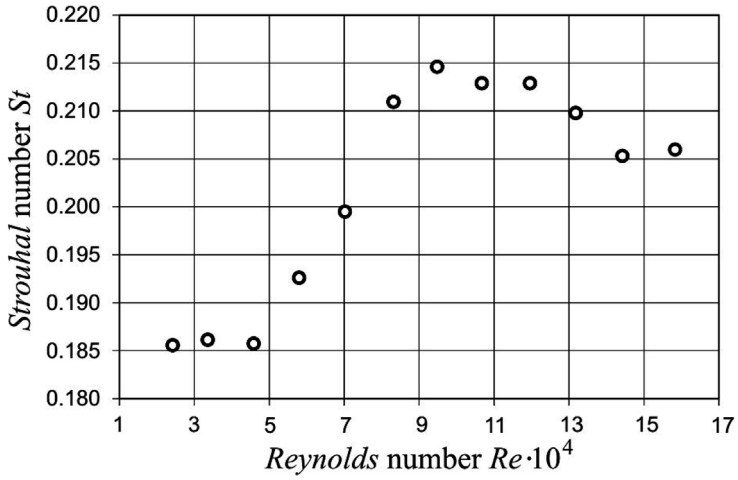

Fig. 17. Variation of the Strouhal number with the Reynolds number for configuration no. 3

8. Conclusions

The experimental creation of the ice on the inclined cable model of cable-supported bridges was carried out in the climatic chamber of the wind tunnel of CET ITAM. The Strouhal number was investigated for the stationary iced cable model with respect to three principal angles of wind attack within the range of the Reynolds number between $2.4 \cdot 10^4$ and $16.4 \cdot 10^4$.

The ice accretion process produced the asymmetrical and irregular iced cross-section of the cable model with rounded edges of ice ribs accreted on the underside of the model (with maximal surface roughness of 18%) and with the quasi-circular shape on its upper part (with minimal surface roughness of 0.73%).

The Strouhal number determined for configuration no. 1 depends on *Re* (Fig. 11). Initially, in the range of $Re = 2.5 \cdot 10^4 – 6.1 \cdot 10^4$, *St* values linear decrease from St = 0.199 to 0.189. In the range of $Re = 6.1 \cdot 10^4 – 9.9 \cdot 10^4$, *St* suddenly increased to St = 0.206 and for $Re > 9.9 \cdot 10^4$, St again decrease to St = 0.198.

The Strouhal number determined for configuration no 2 is changing in the range of St = 0.201 – 0.205 and seems to be independent of *Re* in the range that was studied (Fig. 14). All obtained *St* values are 12% to 14% higher than St = 0.18. The variability of the St values for configuration no. 2 can be incidental and caused by the randomness of the vortex excitation.

The Strouhal number determined for configuration no 3 strictly depends on Re (Fig. 17). St values were initially in the range of St = 0.186 – 0.187 for $Re = 2.4 \cdot 10^4 – 4.6 \cdot 10^4$. In the range of $Re = 4.6 \cdot 10^4 – 9.5 \cdot 10^4$, *St* suddenly increased to a maximum value St = 0.215. In the range of $Re = 9.5 \cdot 10^4 – 15.8 \cdot 10^4$, *St* is in the range of St = 0.205 – 0.215.

It is well known that in the case of the smooth circular cylinder, the studied Reynolds number range is in the subcritical range and the Strouhal number is approximately 0.18. However, previous wind tunnel studies (Zdravkovich, 1997) show that increased surface roughness of the cylinder induces transition to critical and transcritical range at lower Reynolds numbers. Thus, the change effect of the direction of wind acting on the iced cable model on variation of the Strouhal number with the Reynolds number corresponds to experimental data (Zdravkovich, 1997) obtained at different degrees of surface roughness of the cylinder.

This work was created with support from project no. LO1219 under the Ministry of Education, Youth and Sports National sustainability programme 1, and partially with the support from project No. FR-TI3/654 under the Ministry of Industry and Trade. Marcin Tatara is a scholar of a project 'PhD Scholarships - investment in the scientific staff Opole Voivodeship II' co-funded by the European Union within the European Social Fund.

References

[1] Demartino C., Koss H.H., Georgakis C.T., Ricciardelli F., *Effects of ice accretion on the aerodynamics of bridge cables*. Journal of Wind Engineering and Industrial Aerodynamics, Vol. 138, 2015, 98-119.

[2] Eurocode 1, Action on structures – part 1-4: General action – Wind action, 2009.

[3] Flaga A., *Inżynieria wiatrowa*. Arkady, Warszawa 2008.

[4] Flaga A., *Mosty dla pieszych*, WKŁ, Warszawa 2011.

[5] Flaga A., Michałowski T., *Zagadnienia aerodynamiki cięgien w mostach podwieszonych*, Inżynieria i Budownictwo, Vol. 6, 1997, 316-321.

[6] Gjelstrup H., Georgakis C.T., *A quasi-steady 3 degree-of-freedom model for the determination of the onset of bluff body galloping instability*, Journal of Fluids and Structures, Vol. 27, 2011, 1021-1034.

[7] Gjelstrup H., Georgakis C.T., Larsen A., *An evaluation of iced bridge hanger vibrations through wind tunnel testing and quasi-steady theory*, Wind and Structures, Vol. 15(5), 2012, 385-407.
[8] Gurung C.B., Yamaguchi H., Yukino T., *Identification of large amplitude wind-induced vibration of ice accreted transmission lines based on field observed data*. Engineering Structures, Vol. 24, 2002, 179-188.
[9] Hartog J.P.D., *Transmission-line vibration due to sleet*, Institute of Electrical Engineers, Vol. 51, 1932, 1074-1086.
[10] http://cet.arcchip.cz/wind-laboratory-en (online: 07.2014).
[11] http://www.toledoblade.com/gallery/Ice-closes-Skyway (online: 07.2014).
[12] Koss H., Gjelstrup H., Georgakis C.T., *Experimental study of ice accretion on circular cylinders at moderate low temperatures,* Journal of Wind Engineering and Industrial Aerodynamics, Vol. 104-106, 2012, 540-546.
[13] Makkonen L., *Modelling power line icing in freezing precipitation,* Atmospheric Research, Vol. 46, 1998, 131-142.
[14] Zdero R., Turan O.F., *The effect of surface strands, angle of attack, and ice accretion on the flow field around electrical power cables*, Journal of Wind Engineering and Industrial Aerodynamics, Vol. 98, 2010, 672-678.
[15] Zdravkovich M.M., *Flow around circular cylinders, Volume 1: Fundamentals,* Oxford University Press, USA, Oxford 1997.
[16] Zhitao Y., Zhengliang L., Eric S., William E.L., *Galloping of a single iced conductor based on curved-beam theory,* Journal of Wind Engineering and Industrial Aerodynamics, Vol. 123, 2013, 77-87.